

Thermo-Mechanical Analysis for Metallic Fuel Pin under Transient Condition

Dong Uk Lee, Byoung Oon Lee, Yeong Il Kim and Dohee Hahn

Korea Atomic Energy Research Institute

E-mail : dulee@kaeri.re.kr

Abstract — Computational models for analyzing the in-reactor behavior of metallic fuel pins under transient conditions in liquid-metal reactors are developed and implemented in the TRAMAC (TRAnsient thermo-Mechanical Analysis Code) for a metal fuel rod under transient operation conditions. Not only the basic models for a fuel rod performance but also some sub-models used for transient condition are installed in TRAMAC. Among the models, a fission gas release model, which takes the multi-bubble size distribution into account to characterize the lenticular bubble shape and the saturation condition on the grain boundary and the cladding deformation model have been developed based mainly on the existing models in the MACSIS code. Finally, cladding strains are calculated from the amount of thermal creep, irradiation creep, and irradiation swelling. The cladding strain model in TRAMAC predicts well the absolute magnitudes and general trends of their predictions compared with those of experimental data. TRAMAC results for the FM-1,2,6 pins are more conservative than experimental data and relatively reasonable than those of FPIN2 code. From the calculation results of TRAMAC, it is apparent that the code is capable of predicting fission gas release, and cladding deformation for LMR metal fuel under transient operation conditions. The results show that in general, the predictions of TRAMAC agree well with the available irradiation data.

1. Introduction

The precise prediction of the in-reactor fuel performance during transient overpower as well as steady state operation is essential for the design and licensing of liquid metal reactors. Under transient overpower condition fuel temperature is increased^[1]. Exaggerated cladding stresses due to an increased fuel cladding mechanical interaction from the thermal stresses, differential thermal expansion, transient fuel swelling, fuel phase transformation, and incremental gas release may generate a breach of the cladding^[2].

So far, there has been no dedicated computer code for analyzing the in-reactor fuel behavior under the transient condition of KALIMER (Korea Advanced Liquid Metal Reactor), whereas MACSIS (Metal fuel performance Analysis Code for Simulating the In-reactor behavior under Steady-state conditions)^[3] was developed for analyzing the in-reactor behavior and the operation limits of the KALIMER fuel under steady state condition. So TRAMAC (Transient Thermo-Mechanical Analysis Code for Metal Fuel Rod under Transient Operation Condition) has been developed to

simulate the thermo-mechanical behavior of the metal fuel rod under LMR transient operation condition.

Not only the basic models for the fuel rod performance under transient conditions, but also some sub-models are installed in TRAMAC. Among the models, FGR and cladding deformation models have been modified based mainly on the existing models in the MACSIS code. A series of calculations was carried out to provide the swelling contribution of various bubble growth mechanisms that especially included the transient evolution of fission gas bubble distributions on the grain boundaries of the fuel. Existing models in the MACSIS were modified to match the transient conditions, and the models were installed into the TRAMAC code. The TRAMAC code predicts the temperature profile, the stress, and the displacements of the fuel rod under transient conditions such as TOP (Transient overpower), LOF (Loss of flow) etc. The validation of the TRAMAC code results has been performed by comparing with results of EBR-II and Whole Pin Furnace (WPF) test data of the FM-1,2,6 pins^[4].

The objective of this paper is to evaluate thermo-

mechanical behavior for a metal fuel rod with the TRAMAC developed for the KALIMER fuel under transient operation conditions. Section 2 describes the major model descriptions in the TRAMAC code. Section 3 shows the transient scenario and input data for the TRAMAC code. Some preliminary results of the transient modeling and benchmark calculations to evaluate the validity of the TRAMAC are given in section 4. Conclusions are given in the final section.

2. Code Description

2-1. Description of the Transient Deformation Model for a Fuel Slug

All reactor fuels produce volatile fission products as they produce energy. Even though most of the fission gases produced in a fuel matrix are released to the plenum, some are retained within the fuel in the form of bubbles. In the steady-state irradiation, these bubbles achieve an equilibrium condition with the fuel matrix. When the equilibrium between the gaseous bubbles and the fuel matrix is upset by some type of off-normal reactor behavior, the fission-gas bubbles can expand or contract to achieve a new state of equilibrium, and the rate at which they can accommodate the new conditions is related to the creep rate of the fuel matrix^[5].

The gas swelling model considering this phenomenon gives the strain increments and also calculates the fission gas amount released to the gas plenum. This

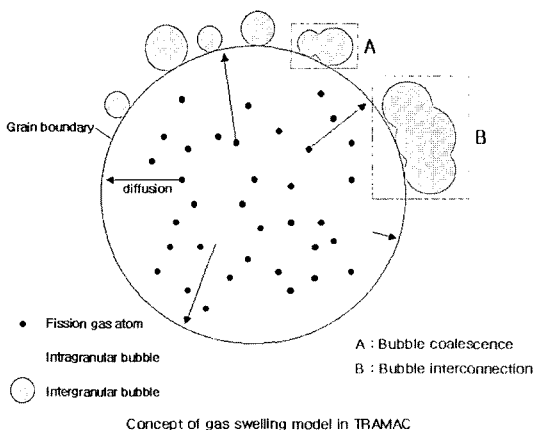


Fig. 1. Concept of the fission gas swelling model in TRAMAC.

swelling model has been incorporated into the TRAMAC code simulating transient condition. The gas swelling model comprises two parts such as Fig. 1. One of the sub-models describes the migration of the fission gas atoms and intragranular gas bubble into the grain or phase boundary. Another model describes the growth of the grain-boundary bubbles.

2-1-1. Intragranular diffusion & solid swelling

In the intragranular fission gas diffusion model, Booths classical diffusion theory^[6] was directly adopted. His approach contains certain basic assumptions; namely that the entire gas content of the material exists as single, freely diffusing atoms, and that the fissioning substance can be considered to consist of discrete homogeneous spherical particles. Since a discontinuity exists at each particle interface, the surface of each spheroid behaves as a perfect sink for the gas atoms. This property defines the boundary condition enabling the solution of the differential equation describing the movement of the fission gas within each sphere, and hence, the calculation of the flux of the gas atoms through each particle surface. The intragranular gas model calculates the amount of gas atoms and bubbles diffusing into the grain boundary.

Also, the solid fission product swelling in the metallic fuel slug can be assumed to be proportional to the local burnup. Hence, the isotropic strain increment $\Delta\epsilon^{sol}$ due to the solid fission product swelling is given in TRAMAC by

$$\Delta\epsilon^{sol} = \dot{\epsilon}^{sol} \cdot \Delta Bu \quad (1)$$

where $\dot{\epsilon}^{sol}$ is the volumetric strain increment per atomic percent burnup (at.%) due to the solid fission products swelling, and ΔBu is the burnup increment.

The solid fission products swelling rate was determined from the calculation of the volume of all the solid and liquid fission products^[7]:

$$\dot{\epsilon}^{sol} = 1.26\%/at.\% \quad (2)$$

2-1-2. Intergranular bubble behavior & gaseous swelling

The gaseous swelling on the grain boundary is a major component of the fuel swelling mechanism. In general, the fuels with a high thermal conductivity exhibit a high fission-gas-induced swelling. This consists of the nucleation and growth of largely immobile

intragranular bubbles, and through the diffusion of fission gas to the grain boundaries, in relatively larger intergranular bubbles. At a sufficient fissile burnup, intergranular bubbles link up and form paths for fission gas release from the fuel. Intragranular bubbles may eventually grow large enough to interconnect as well. At this point, a large amount of swelling has occurred, and therefore, a major fraction of the fission gas will be released from the fuel. Allowing a large amount of fuel swelling and gas release to take place reduces fuel-cladding mechanical interaction (FCMI), and is the key to successful high burnup operation of fuels^[5]. While intragranular bubbles achieve an equilibrium condition with the fuel matrix under normal condition, these do not maintain an equilibrium between the fuel matrix and internal pressure within the bubbles under off-normal condition. This phenomenon under transients reduces the fission gas atom density within the bubbles, and finally volume of the fuel is rapidly expanded.

The gaseous swelling amount can be estimated by taking the multi-bubble size distribution and the saturation condition on the grain boundary into account.

As described in the reference^[3], the multi-bubble size distribution on the grain boundary and the average number of bubbles per unit volume at a given *i* bubble size range, \bar{f}_i , is estimated by:

$$\int_{n_i}^{n_{i+1}} F(m, \tau, n) dn = \bar{f}_i (n_{i+1} - n_i)$$

or:

$$\bar{f}_i (n_{i+1} - n_i) = 0.23 m \cdot \tau^{-4.5} \int_{n_i}^{n_{i+1}} \{ \exp(-A(n\tau^{-2.5} - 0.5)) \} \times \{ \sinh[B(n\tau^{-2.5} - 0.5)]^{1/2} \} dn \quad (3)$$

where, n_i =number of gas atoms in the *i* size bubble, τ =reduced time as a dimensionless parameter, $m' = m_{gb}/E_i$, the number of gas atoms per unit volume around the grain boundary surface, m_{gb} =number of gas atoms per unit area on the grain boundary, E_i =the effective thickness of the grain boundary, A, B= dimensionless constants, -0.7 and 1.12 respectively.

As described in the reference^[8], the saturation condition on the grain boundary is estimated by:

$$\frac{\pi}{4} = \sum_{\text{size range}} (r_{ib,i})^2 \cdot f_i \quad (4)$$

where, $r_{ib,i}$ =longer radius of the *i* size lenticular bubble on the grain boundary, f_i =equivalent number of bubbles at the *i* size range.

Gas retained in the fuel during steady-state irradiation provides a source for expansion of both the solid and liquid fuel during overheating. The quantity of fission gas in the plenum is also important because the plenum pressure is a major contributor to the cladding loading and, therefore, to a cladding failure. In TRAMAC, the gas increased in the plenum is applied with a multi bubble size distribution on the grain boundary based on the WPF tests.

2-1-3. The model of the fuel swelling

The fuel swelling is primarily due to the retained fission gas bubbles on the grain boundary and the solid fission product accumulation within the matrix, including the liquid phase product. The sum of the volumes of the bubbles trapped on the grain boundary under transient operation condition is determined by considering the transient high temperature profile, and the fractional swelling under transient condition is calculated. Finally, swelling caused by solid fission products is added to obtain the total fission-induced swelling. These two mechanisms are incorporated into TRAMAC as follows.

A gas bubble tends to maintain an equilibrium gas pressure by balancing the internal gas pressure against the bubble surface tension and the external pressure. The van der Waals gas law is used to calculate the fission gas swelling. The bubble sizes are defined according to the number of gas atoms. The bubble radius r_i is given by reference^[8]:

$$r_i = [(3kT/8\pi\gamma)n_i]^{1/2} \quad (5)$$

where γ is surface tension of metal fuel, 0.8 J/m², k is Boltzmann constant, T is temperature (K), n_i is number of gas atoms in the *i* size bubble.

The volume change of the fuel slug due to a gas swelling is calculated to take into account the multiple-bubble size distribution on the grain boundary. The fractional volume increase due to the accumulation of the gas bubbles is given by:

$$\Delta V_s = \sum_{j=1}^{10} \left\{ \left[\frac{4}{3} \pi n_{i,j} \sum_{i=1}^{10} r_{i,j}^3 \right] V_j \right\} + f_s \quad (6)$$

where, V_j is the volume of *j* annulus, $n_{i,j}$ is the num-

ber of bubbles in the i size bubble at the j annulus, $r_{i,j}$ is the radius of the i size bubble at the j annulus, f_v is the fractional volume change due to the buildup of the solid fission products.

Therefore, the fractional increase in the fuel radius due to a fuel swelling is given by

$$\Delta D_s \cong r_0 \left\{ \frac{0.5 \Delta V_s}{V_0} \right\} \quad (7)$$

where, r_0 is the radius of the fuel core, V_0 is the initial volume of the fuel core.

2-2. Description of the Cladding Deformation Model

The deformation of the cladding during transients can be produced by a mechanical loading and by a metallurgical interaction with the fuel. The primary sources of a mechanical loading come from fission the gas plenum pressure and the Fuel-Cladding Mechanical Interaction (FCMI). Gas pressure loading is dominant for a low burnup fuel where the fuel-cladding gap has not closed and for undercooling transients where the cladding tends to expand away from the fuel. FCMI loading of the cladding can occur under Transient Over Power (TOP) conditions where the fuel expands into the cladding. However certain characteristics of metallic fuels tend to minimize this effect. Namely, FCMI can be avoided for a high burnup if the as-built smeared density is kept to 75%. These characteristics include the similarities in the thermal expansion coefficients between the fuel and the cladding. In addition, the greatest transient cladding deformation usually occurs at the axial location where the cladding temperatures are the greatest. This occurs near the top of the fuel column where, in metallic fuel pins, the fuel stresses tend to relax to a hydrostatic state in an equilibrium with the plenum pressure^[4]. Up to a burnup of 18 at.% in the metallic fuel, it appeared that any contribution to the cladding strain from the fuel/cladding mechanical interaction was insignificant. This may be too simplistic for a precise evaluation of FCMI, but it appears adequate for an analysis of the both steady-state and transient performance^[9]. Therefore the predicted major cladding strains under transients are the mechanical creep strain caused by a differential thermal expansion of the fuel and

cladding, irradiation-induced creep strain, and the irradiation swelling of the cladding itself.

The fuel thermal expansion is computed by finding the volumetric average radial displacement. At each radial node the displacement is computed using the coefficient of the thermal expansion given by

$$\alpha' = \alpha_0' + \alpha_T' \times T \quad (8)$$

The thermal expansion of the cladding material (HT9) is computed from the linear function of the temperature in the open gap.

$$\frac{\Delta L}{L} = (\alpha_0^c + \alpha_T^c T)(T - T_R) \quad (9)$$

where T_R is the room temperature, T is the average cladding temperature, and $\Delta L/L$ is the fraction of the length change.

An in-reactor creep equation for HT9 was used as the rate form; $\dot{\epsilon} = \dot{\epsilon}_i + \dot{\epsilon}_T$, the terms $\dot{\epsilon}_i$ and $\dot{\epsilon}_T$ are the irradiation-induced and thermal creep terms of equation respectively^[10]. The rate form of the creep equation is given, as follows.

$$\dot{\epsilon}_i = \left[B_0 + A \exp\left(-\frac{Q}{RT}\right) \right] \phi \bar{\sigma}^{1.3} \times 10^{-7} \quad (10)$$

where $\bar{\epsilon}_i$: effective strain (%), $\bar{\sigma}$: effective stress (MPa), Q : activation energy, T : temperature (K), R : gas constant, ϕ : neutron fluence (10^{22} n/cm², $E > 0.1$ Mev)

$$\dot{\epsilon}_T = \dot{\epsilon}_{TP} + \dot{\epsilon}_{TS} + \dot{\epsilon}_{TT} \quad (11)$$

Below 600°C

$$\begin{aligned} \dot{\epsilon}_{TP} &= \left[C_1 \exp\left(-\frac{Q_1}{RT}\right) \bar{\sigma} + C_2 \exp\left(-\frac{Q_2}{RT}\right) \bar{\sigma}^4 \right. \\ &\quad \left. + C_3 \exp\left(-\frac{Q_3}{RT}\right) \bar{\sigma}^{0.5} \right] C_4 \exp(-C_4 t) \\ \dot{\epsilon}_{TS} &= C_5 \exp\left(-\frac{Q_4}{RT}\right) \bar{\sigma}^2 + C_6 \exp\left(-\frac{Q_5}{RT}\right) \bar{\sigma}^5 \\ \dot{\epsilon}_{TT} &= 4C_7 \exp\left(-\frac{Q_6}{RT}\right) \bar{\sigma}^{10} t^3 \end{aligned} \quad (12)$$

For a higher temperature

$$\begin{aligned} \dot{\epsilon}_{TP} &= \left[C_1 \exp\left(-\frac{Q_1}{RT}\right) \bar{\sigma} + C_2 \exp\left(-\frac{Q_2}{RT}\right) \bar{\sigma}^4 \right. \\ &\quad \left. + C_3 \exp\left(-\frac{Q_3}{RT}\right) \bar{\sigma}^{0.5} \right] C_4 (1 - \exp(-C_4 t)) \end{aligned}$$

$$\begin{aligned}\dot{\epsilon}_{TS} &= \left[C_5 \exp\left(-\frac{Q_4}{RT}\right) \bar{\sigma}^2 + C_6 \exp\left(-\frac{Q_5}{RT}\right) \bar{\sigma}^5 \right] t \\ \dot{\epsilon}_{TT} &= C_7 \exp\left(-\frac{Q_6}{RT}\right) \bar{\sigma}^{10} t^4\end{aligned}\quad (13)$$

where $\dot{\epsilon}_{TP}$: thermal primary creep strain rate (%/s),
 $\dot{\epsilon}_{TS}$: thermal secondary creep strain rate (%/s), $\dot{\epsilon}_{TT}$:
thermal tertiary creep strain rate (%/s), $\bar{\sigma}$: effective
stress (MPa), t : time in seconds.

Values for the constants in these equations are :

$$R=1.986 \text{ cal}^\circ\text{K mole (gas constant)}$$

$$B_0=1.38 \times 10^{-4}$$

$$A=2.59 \times 10^{14}$$

$$Q=73,000$$

$$C_1=13.4,$$

$$C_2=8.43 \times 10^{-3} \quad Q_1=15,027$$

$$C_3=4.08 \times 10^{18} \quad Q_2=26,451$$

$$C_4=1.6 \times 10^{-6} \quad Q_3=89,167$$

$$C_5=1.17 \times 10^9 \quad Q_4=83,142$$

$$C_6=8.33 \times 10^9 \quad Q_5=108,276$$

$$C_7=9.53 \times 10^{21} \quad Q_6=282,700$$

Swelling is generally the function of the fluence and expressed in a bilinear equation. HT9 may never show a significant swelling, regardless of the fluence, although a transmission electron microscopy has revealed a few voids at a low temperature ($\sim 400^\circ\text{C}$)^[7].

$$\frac{\Delta V}{V} = S_0 + A \quad (14)$$

where S_0 is the fractional volume change due to the void formation and A is the fractional volume change due to the solid state reactions.

$$S_0 = (0.01)R \left[\phi t + \frac{1}{\alpha} \ln \left\{ \frac{1 + \exp[\alpha(\tau - \phi t)]}{1 + \exp(\alpha\tau)} \right\} \right]$$

$$A = (0.01)(0.15)[1 - \exp(-0.1\phi t)] \quad (15)$$

$$\begin{aligned}\text{where } R &= 0.085 \exp[-1 \times 10^{-4}(T-400)^2], \\ \tau &= 14.2, \quad \alpha = 0.75(10^{22} \text{ n/cm}^2)^{-1}, \\ \phi t &= 10^{22} (\text{n/cm}^2)^{-1}\end{aligned}$$

3. Transient Scenario and Input Data

This study will concentrate on the cladding deformation and its integrity, which are of a fundamental concern because the cladding provides the primary barrier to the release of radionuclides. Cladding damage during accident transients is a strong function of the cladding temperature. For design basis accident (DBA) transients including the scram-protected transient overpower (TOP), loss-of-flow (LOF) and loss-of-heat sink (LOHS) events, the thermal response of the cladding for these transients can generally be characterized by a temperature ramp of 1~100°C/s followed by a reactor scram and a rapid cooling within 10~20 seconds after accident initiation^[4].

One of the key phases in the development of the code for analyzing a transient fuel behavior is the validation of the code's predictions through a comparison of the calculated results with the results of experiments on metallic fuels. Tests on intact transient fuel pins include in-reactor tests in the EBR-II reactor, and the out-of-reactor Whole Pin Furnace (WPF) test which has been developed to span the range between the TREAT and the EBR-II test regimes.

Six WPF tests have been conducted using IFR metallic fuel pins irradiated in EBR-II. Key pin parameters and test conditions for the FM-1,2,6 pins are summarized in Table 1. The fuel characterization such as the geometry, fission gas release, fuel restructuring, based on the calculation of MACSIS which is a computer program for simulating the behavior of the metal fuel rods for a liquid metal cooled reactor under normal operating conditions for the test pin, are inputted into the TRAMAC. The TRAMAC also needs

Table 1. Test condition for FM-1,2,6 rod and test results.

Test no.	Fuel type	Cladding type	Plenum fuel vol. ratio	Burnup (a/o)	Test temp. (°C)	Test duration (min)	Failure time (min)	Peak strain (%)
FM-1	U-10Zr	HT9	1.0	3.0	820	67	67	3.3
FM-2	U-19Pu-10Zr	HT9	1.0	3.0	820	112	112	2.3~4.3
FM-6	U-19Pu-10Zr	HT9	1.0	11.3	650~670	2160	No failure	0.89

the simulated cladding surface temperatures based on the peak cladding temperature and the axial temperature profile determined from furnace tests. And then, the TRAMAC calculates the thermal-mechanical phenomena, which govern fuel and cladding behavior during transient.

FM-1 and FM-2 experiments were ramp-and-hold tests with the peak-cladding temperature ramped from 500°C to the test temperature at 6°C/s, followed by a hold at the test temperatures (820°C) until the signal of the fuel pin failure was detected. Also test FM-6 was run in two stages of a ramp-and-hold test at nominal peak cladding temperatures of 650~670°C (650°C at the fuel top, 670°C in the plenum). Stage 1 of the test was run for 12 hours, just after which the pin was removed from the test section to measure the incremental diametral strains. The pin was then inserted back into the furnace and run for another 24 hours.

4. Benchmark Calculation and Discussion

To evaluate the predictive capability of TRAMAC, we need to compare the calculation results of fission gas release and the cladding strain by TRAMAC with the WPF experimental results. For the comparison of the predictions for the cladding deformation with the experimental data, the test results for the FM-1,2,6 test rods were used, which were irradiated at the Experimental Breeder Reactor II by ANL until 3, 11.3 at.% and then have conducted test at WPF (Whole Pin Furnace). The WPF testing facility uses a computer-controlled radiant furnace, which is able to heat intact irradiated fuel pins up to the temperature point of the cladding breach.

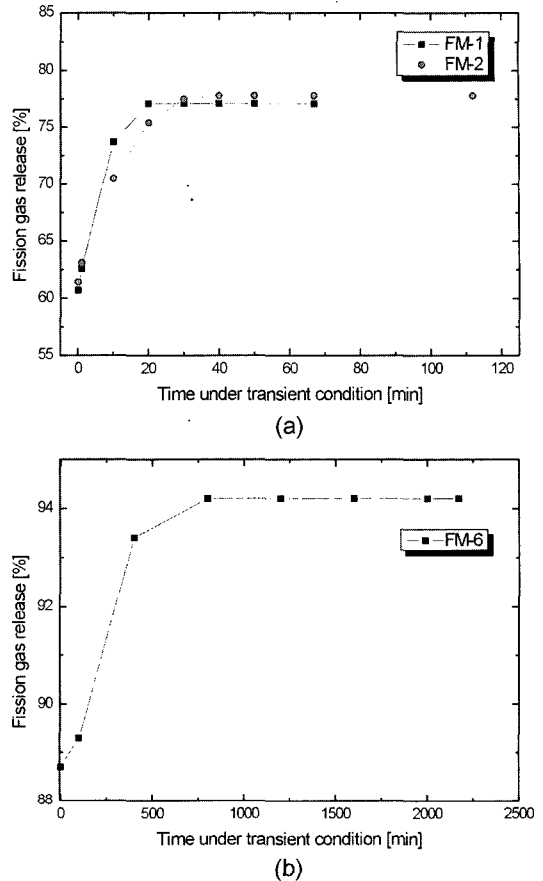


Fig. 2. a. FGR of FM-1,2, b. FGR of FM-6.

The fission gas release evaluated with the multi bubble size distribution is shown in Figs. 2a, b respectively. However these values are based not on the transient fission gas release model but the WPF failure cladding strain data.

The comparisons of the calculation and test results

Table 2. Comparison of the calculation and test results.

	FM-1		FM-2		FM-6	
	Peak strain (%)	Time (min)	Peak strain (%)	Time (min)	Peak strain (%)	Time (min)
FPIN2	6	36***	6	42	6	270
LIFE	1.1	79*	~1	75	1.03	1320**
TRAMAC	4.59	67	5.946	~49	1.42	2174
TEST	3.3	67	2.3-4.3	112	0.89	2160

*Transient creep-rupture correlation.

**Steady-state creep-rupture correlation.

***6% cladding strain criterion based on transient plastic flow law.

are summarized in Table 2. The calculated cladding failure times are based on various failure criteria contained within the codes. The 6% cladding strain criterion is based on data from the FCTT transient tube burst tests¹⁴. For FM-1, Fig. 3a shows a cladding strain during normal operation of 120 days and also shows a strain up to transient operation of 67 minutes after the normal operation. The TRAMAC predicted peak cladding strain is 4.59%. The prediction by TRAMAC is higher than that of experimental data (3.3%). This result is more conservative than the experimental data with the failure time (67 min). However, it is apparent that the prediction by the TRAMAC code is in slightly better agreement with the experiments than that (6%) of FPIN2. Based on the transient plastic flow law, 6% of a strain can be applied as a strain criterion of the fuel rod under tran-

sient condition. According to this criterion, the FPIN2 exceeded the criterion at only 36 minutes and the fuel pin was failed.

For FM-2, it appears that the TRAMAC result exceeds the peak strain of 6% within about 50 minutes as shown in Fig. 4a. This result is also more conservative than the experimental data (4.3%) with the failure time of 112 minutes. FPIN2 predicts only 42 minutes of time to a fail, which is much lower than that of the experiment data. For FM-6, Fig. 5a shows a cladding strain during normal operation of 470 days and it also shows a strain up to transient operation of 2160 minutes after a normal operation. The TRAMAC predicted peak cladding strain is 1.42% during 2174 minutes as shown in Fig. 5a. This result is also more conservative than the experimental data (0.89%) without a failure during 2160 minutes.

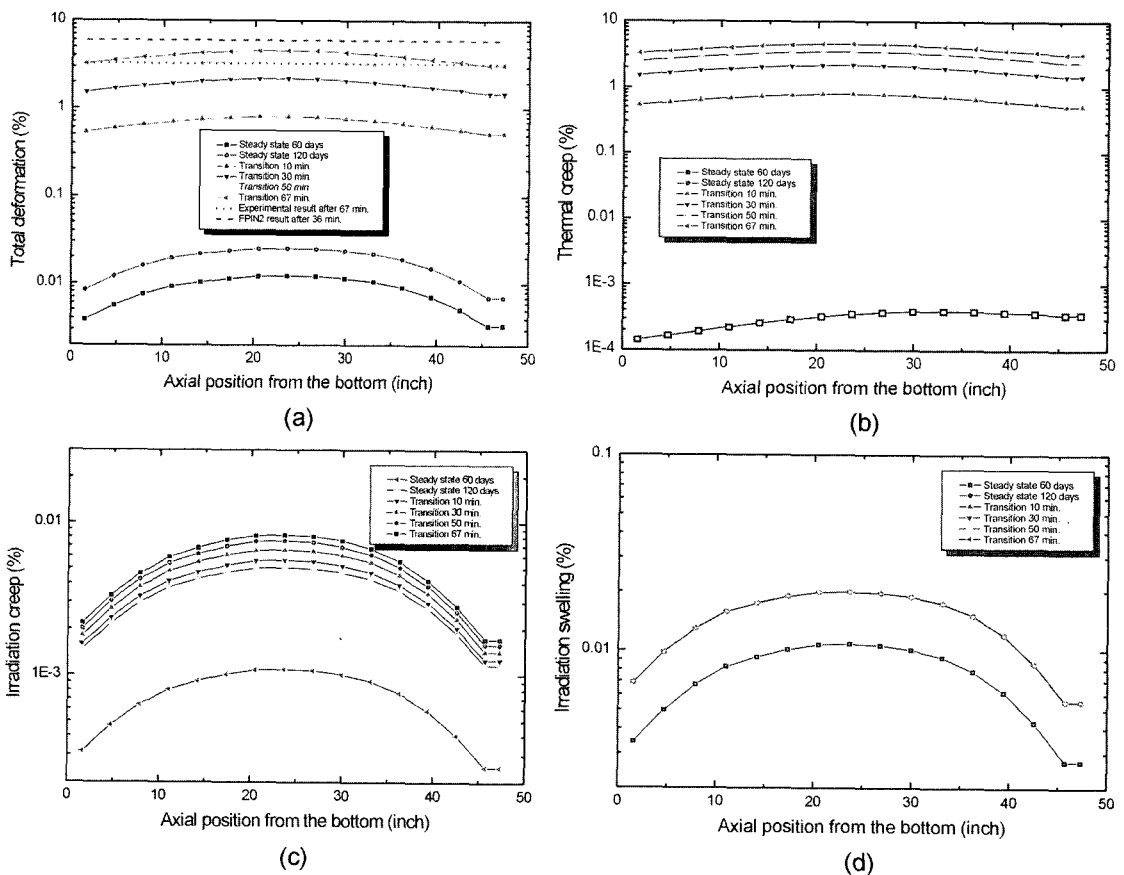


Fig. 3. a. Total cladding strain for the FM-1 rod, b. Thermal creep for the FM-1 rod, c. Irradiation creep for the FM-1 rod, d. Cladding irradiation swelling for the FM-1 rod.

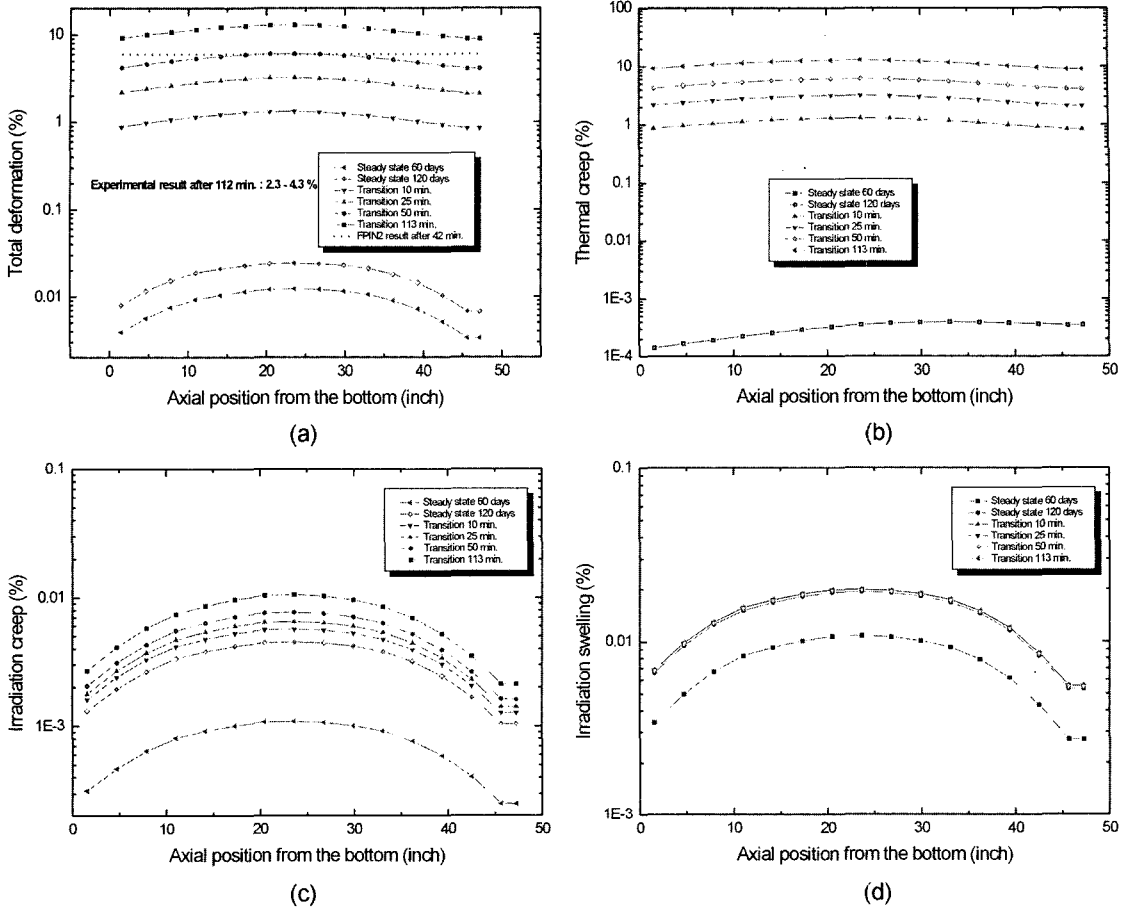


Fig. 4. a. Total cladding strain for the FM-2 rod, b. Thermal creep for the FM-2 rod, c. Irradiation creep for the FM-2 rod, d. Irradiation cladding swelling for the FM-2 rod.

FPIN2 predicts only 270 minutes of time to a fail, which is much lower than that of the experiment data.

For irradiation temperatures less than 540°C, as in-reactor creep data are consistent with a stress exponent of $1 \leq n < 2$, creep is relatively insensitive to temperature but sensitive to the temperature range higher than 570°C. And for the temperature range higher than 650°C, HT9 alloy no longer displays the in-reactor creep resistance exhibited at irradiation temperatures less than 570°C, since the HT9 in-reactor creep increases with a stress exponent of the order 3 to $7^{[12]}$. Therefore as shown in the Fig. 3b~d, 4b~d and 5b~d, total cladding strain is affected by irradiation swelling with a linear fluence dependence because the cladding temperatures are less than 650°C under steady-

state condition. When cladding temperature exceeds 650°C under transient condition, the thermal creep mechanisms dominate the in-reactor creep behavior of the HT9.

As stated above, the TRAMAC results for the FM-1,2,6 pins are in slightly better agreement with the experiments than those of the FPIN2. The predictions of TRAMAC are more conservative than experimental data and more relatively reasonable than those of the FPIN2. In other words, TRAMAC predicted shorter failure times and slightly larger plastic strains than the experimental data. The cladding strains predicted by TRAMAC seem to agree well with the trend. The foregoing comparisons show that TRAMAC is capable of efficiently simulating the in-reactor behavior of a metallic fuel under transient events.

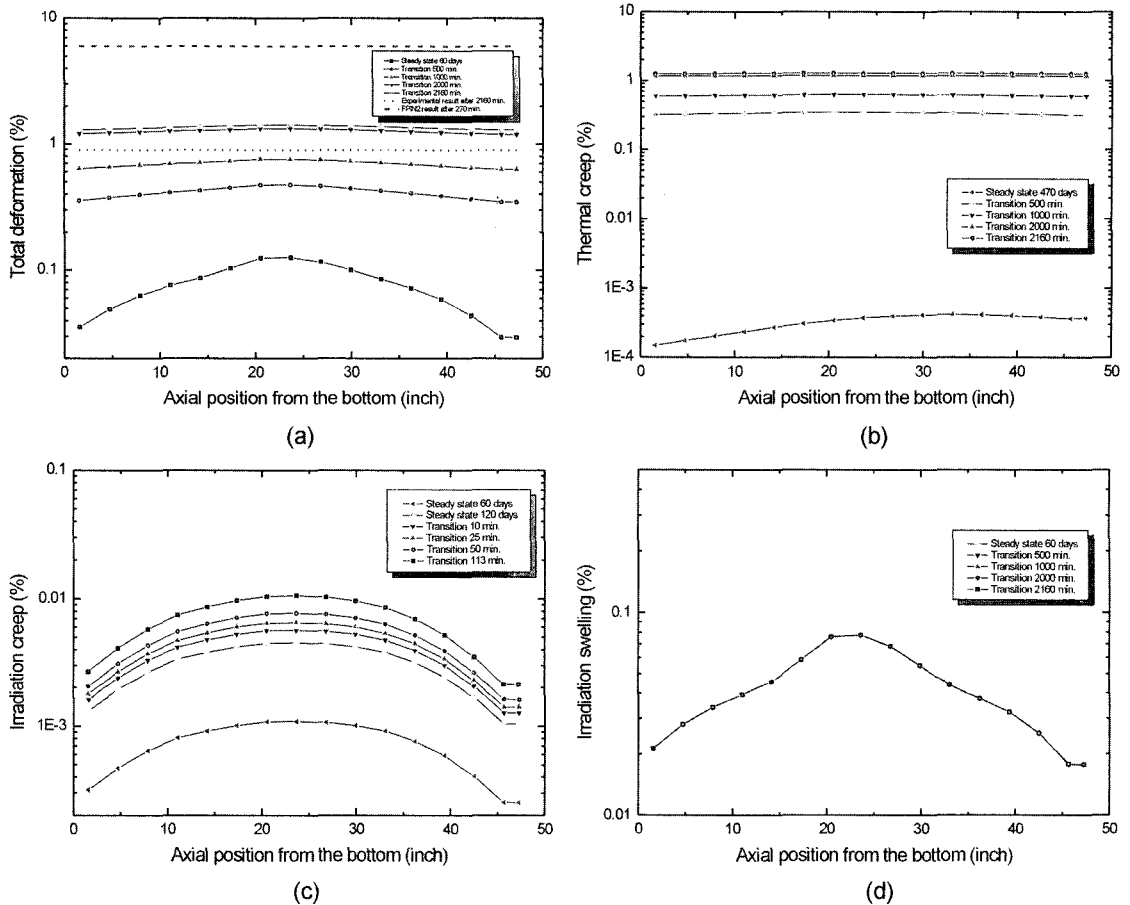


Fig. 5. a. Total cladding strain for the FM-6 rod, b. Thermal creep for the FM-6 rod, c. Irradiation creep for the FM-6 rod, d. Irradiation cladding swelling for the FM-6 rod.

5. Conclusions

The precise prediction of the in-reactor fuel performance during transient overpower as well as a steady state operation is essential for the design and licensing of liquid metal reactors.

The TRAMAC for simulating transient in-reactor behavior of a fuel rod has been successfully modified for a metal fuel in KALIMER. Not only the basic models for the fuel rod performance, but also some sub-models used for a transient condition are installed in TRAMAC. Among the models, the semi-theoretical fission gas release and cladding deformation models have been modified based mainly on the existing models in the MACSIS code. The validation of the TRAMAC code was evaluated by comparing the pre-

dictions with the available experimental data.

The cladding strain model in TRAMAC predicts well the absolute magnitudes and the general trends of their predictions when compared with those of the experimental data. From the calculation results of TRAMAC, it is apparent that the code is capable of predicting the fission gas release, and the cladding deformation for a LMR metal fuel under transient condition. Therefore, the general potential of TRAMAC as a calculational tool to evaluate the integrity of a metal fuel under transient operation conditions is identified.

Acknowledgement

This study was supported by the Korean Ministry

of Science & Technology through its National Nuclear Technology Program.

References

1. Roth, T.S. and Biancheria, A.: "A Model to Predict The Failure of Liquid-Metal-Reactor Fuel Pins During Transient Overpower Conditions", Proceeding ANS International Conference on Reliable Fuels for LMRs (1986).
2. Cahn, R.W. *et al.*: Material Science and Technology, Volume 10 A, Nuclear Material Part I. VCH Publishers Inc., New York (1994).
3. Hwang, W. *et al.*: "MACSIS : A Metallic Fuel Performance Analysis Code for Simulating In-reactor Behavior under Steady-state Conditions", Nuclear Technology, 123, 130, (1998).
4. Kramer, J.M. *et al.*: "Modeling The Behavior of Metallic Fast Reactor Fuels During Extended Transients", J. Nucl. Mater. 204, 203 (1993).
5. Hofman, G.L. *et al.*: "Swelling Behavior of U-Pu-Zr", Metallurgical Transactions A, 21A, 517 (1990).
6. Booth, A.H.: "A Method of Calculating Fission Gas Diffusion from UO₂ Fuel and Its Application to the X-2-f Loop Test", CRDC-721, Atomic Energy of Canada Limited (1957).
7. Hwang, W. *et al.*: "Deformation Analysis on HT-9 Fuel Rod According to The Variations of Temperature and Neutron Flux", Proceedings of the Korean Nuclear Society Spring Meeting, Korea (1998).
8. Hwang, W. *et al.*: "A Comprehensive Fission Gas Release Model Considering Multiple Bubble Sizes on The Grain Boundary under Steady-state Conditions", Nuclear Technology, 95, 314 (1991).
9. Hofman, G.L. *et al.*: "Metallic Fast Reactor Fuels", Progress in Nuclear Energy, 31, 83 (1997).
10. Kim, S.H. *et al.*: "State-of-the-Art Report on Liquid Metal Reactor Core Material HT9", KAERI/AR-493/98, Korea Atomic Energy Research Institute (1998).
11. Gelles, D.S.: "Swelling in Several Commercial Alloys Irradiated to Very High Neutron Fluence", J. Nucl. Mater., 122&123, 207 (1984).
12. Puigh, R.J. and Wire, G.L.: "In-reactor Creep Behavior of Selected Ferritic Alloys", Topical Con. On Ferritic Alloys for Use in Nuclear Energy Technology, Utah, USA (1983).